

## Band gaps in some group-IV materials: A theoretical analysis

Jennifer L. Corkill and Marvin L. Cohen

*Department of Physics, University of California at Berkeley, Berkeley, California 94720  
and Materials Sciences Division, Lawrence Berkeley Laboratory, Berkeley, California 94720*

(Received 9 November 1992)

We have studied the effects of expansion of the lattice on band-edge levels in Si, Ge, Sn, and SiSn. The variation in the gap in the Si→Ge→Sn series can be explained as moving along a universal curve of the variation of band-edge levels with the combined effect of volume and potential. For all of the materials studied, the gap at low volumes is from  $\Gamma$  to  $X$ . There is a small range of volumes where the gap is from  $\Gamma$  to  $L$ , and at high volumes the gap is direct until it closes. Thus, in addition to the usual process of applying positive pressure to close the gap, applying negative pressure also causes band overlap and metallization.

### INTRODUCTION

Because of recent observations of photoluminescence in porous silicon<sup>1</sup> there has been a revival of interest in ways to create a silicon structure with a direct band gap. The widespread technological use of silicon has provided a wealth of information about this material. A direct gap semiconductor based on existing silicon technology is highly desirable since the silicon information base would likely provide direction in solving problems from design to processing.

In addition to the motivation of examining the possible production of Si with a direct band gap, the purpose of this study is to understand the trends in band gaps of group-IV materials. Going down the group-IV column, the band-structure changes tend to produce a direct gap material. However, for  $\alpha$ -Sn the gap at  $\Gamma$  goes to zero. A material intermediate between Ge and Sn could possibly give a moderate direct gap. The advantage of high carrier mobilities in nonpolar, direct gap materials would also make a IV-IV alloy intermediate between Ge and Sn of technological interest.

Theoretical efforts for predicting group-IV materials that are likely to have direct gaps have been concentrated in two areas. The first is the investigation of materials where the cubic symmetry is broken and the zone-edge states are folded back to the center of the zone as in the models of porous silicon,<sup>2</sup> and Si-Ge superlattices.<sup>3</sup> The second area focuses on predicting the properties of IV-IV alloys with the diamond structure.<sup>4</sup> This in effect alters the chemical and structural environment of the bulk material in a uniform way. Here we consider the latter approach and attempt to provide a theoretical base for further studies of these materials.

The chemical trends in group-IV compounds were studied previously<sup>5</sup> using a simplified pseudopotential model. It was shown that at a fixed lattice constant ( $a_0$  for Ge) one could reconstruct the characteristic features of the electronic structure of the Ge→Sn→Pb series by simply varying one Fourier component of the pseudopotential.

To study the variations in the types and sizes of band gaps of the group-IV and IV-IV materials, we have cal-

culated the energy levels at high-symmetry points as a function of primitive cell volume for Si, Ge, Sn, and SiSn (in the zinc-blende structure). We consider the effects arising from the increase in volume with no change in potential. This is a complimentary study to that done in Ref. 5 where the effects of a change in potential were studied. It is found that unit-cell size and variations in the potential give similar changes in the band structures of these materials.

### METHOD

In this study the self-consistent charge densities and eigenvalues are obtained by solving the one-particle Schrödinger equation. *Ab initio* pseudopotentials<sup>6</sup> are used to represent the electron-ion interaction and the exchange and correlation interaction is given by the potential derived<sup>7</sup> from the Monte Carlo calculations of Ceperley and Alder<sup>8</sup> within the local-density approximation (LDA). The Sn pseudopotential includes scalar-relativistic effects, whereas the Si and Ge potentials are nonrelativistic. The Kohn-Sham equations are solved using a plane-wave basis with an energy cutoff of 30 Ry. The charge density and potentials are represented by Fourier components up to  $G_{\max} = \max\{|\mathbf{G}|\} = 10.95 \text{ a.u.}^{-1}$ . Ten special  $\mathbf{k}$  points<sup>9</sup> are used to sample the Brillouin zone with occupation of the valence-band states only. This does not pose a problem for determining the potential because of partial band occupation since even for the calculations of Sn at high volume there is band overlap over a very small fraction of the Brillouin zone.

The LDA does not accurately describe the eigenvalues of the electronic states which causes quantitative underestimations of band gaps. However, the pressure derivatives of conduction-band states<sup>10</sup> and their relative positions are given reasonably well within the LDA. We therefore assume that the band states calculated within the LDA show the qualitatively correct ordering and dependence on cell volume.

In order to investigate the effects of cell volume on the size of the energy gap and position of the conduction-band minimum of the group-IV materials the total band energy  $\epsilon_{\mathbf{k}}$ , the (local) potential energy, and the kinetic

energy at selected symmetry points as a function of cell volume are examined. To calculate the potential energy  $U_{\mathbf{k}}$  of a state  $\mathbf{k}$ ,

$$U_{\mathbf{k}} = \int_{\Omega} \rho_{\mathbf{k}}(r) V_{\text{tot}}(r) d^3r = \Omega \sum_{\mathbf{G}} \rho_{\mathbf{k}}(\mathbf{G}) V_{\text{tot}}(-\mathbf{G}) \\ = \Omega \sum_{\mathbf{G}} \rho_{\mathbf{k}}(\mathbf{G}) V_{\text{tot}}^*(\mathbf{G}), \quad (1)$$

we use the Fourier components  $V(\mathbf{G})$  of the self-consistent potential and  $\rho_{\mathbf{k}}(\mathbf{G})$  of the charge density. The kinetic energy is given by

$$T_{\mathbf{k}} = \Omega \sum_{\mathbf{G}} |a_{\mathbf{k}}(\mathbf{k} + \mathbf{G})|^2 (\mathbf{k} + \mathbf{G})^2 \quad (2)$$

where  $a_{\mathbf{k}}(\mathbf{k} + \mathbf{G})$  is defined by

$$\psi_{\mathbf{k}}(\mathbf{r}) = \sum_{\mathbf{G}} a_{\mathbf{k}}(\mathbf{k} + \mathbf{G}) e^{i(\mathbf{k} + \mathbf{G}) \cdot \mathbf{r}}. \quad (3)$$

The total band energy  $\epsilon_{\mathbf{k}}$  includes a contribution from the nonlocal parts<sup>11</sup> of the potential in addition to  $T_{\mathbf{k}}$  and  $U_{\mathbf{k}}$ . This nonlocal term can be a large fraction of  $\epsilon_{\mathbf{k}}$  (about 2 eV for the  $\Gamma_{25'}$  state in Si at  $V_0$ ), but does not vary as much as  $T_{\mathbf{k}}$  or  $U_{\mathbf{k}}$  with volume.

## RESULTS AND DISCUSSION

### Silicon

First we study silicon as a prototype for the group-IV elemental semiconductors. In Fig. 1 the variation in the one electron energy levels at the top of the valence band and at several high-symmetry points in the conduction band is shown. At the equilibrium volume, the band gap is indirect from  $\Gamma$  to  $\Delta$  85% along the line from  $\Gamma$  to  $X$ . The energy dependence of the state at  $X$  closely follows the minimum along  $\Delta$ ; therefore, for simplicity the  $X$  band edge is plotted instead of the minimum.

Although the minimum direct gap in Si is from  $\Gamma_{25'}$  to the  $\Gamma_{15}$  level at  $V_0$ , the dependence of the  $\Gamma_{15}$  level on volume (pressure) is small. It is the next  $\Gamma$  state,  $\Gamma_{2'}$ , which changes most rapidly with an increase in cell volume and is therefore of interest in this study.

The indirect gap first increases with volume until the  $L_1$  state crosses the  $X_1$  state. Then for a small range of volumes the gap is from  $\Gamma_{25'}$  to  $L_1$  which is similar to Ge at zero pressure. At around 355 a.u.<sup>3</sup> the LDA gap becomes direct, from  $\Gamma_{25'}$  to  $\Gamma_{2'}$  and finally closes at around 370 a.u.<sup>3</sup> per cell. Above 370 a.u.<sup>3</sup>, the gap is zero because of the threefold degeneracy of the  $\Gamma_{25'}$  state, similar to Sn. So, in a qualitative way, the trend of the band levels with volume in Si mimics the trend in the group-IV elements from Si→Ge→Sn.

For Si, there exists a range of volumes where the gap is direct. The volume at which the gap becomes direct, however, corresponds to a negative pressure of about 155 kbar, much larger than the predicted -69 kbar (Ref. 12) required to stabilize Si in the graphite phase. One approach to achieving a larger volume is to grow several layers of Si on a substrate which forces the crystal to

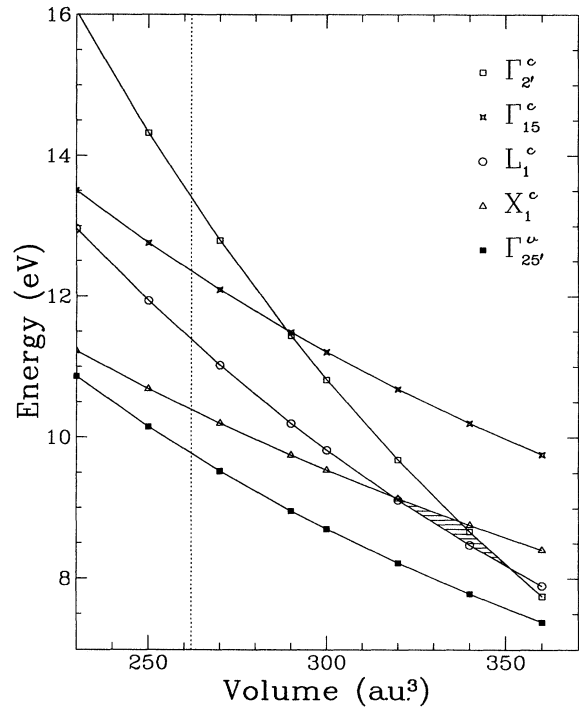


FIG. 1. Band-edge levels as a function of the primitive cell volume for Si are shown. The calculated equilibrium volume is denoted by the dashed vertical line. States are labeled as valence- or conduction-band states based on their positions at the equilibrium volume. The shaded triangle is discussed in the text.

have a large lattice constant. However a suitable substrate is not obvious since InSb ( $V_0 \sim 341$  a.u.<sup>3</sup>) is not large enough and Sn ( $V_0 \sim 460$  a.u.<sup>3</sup>) is opaque. It is also likely that on any substrate the highly strained lattice would relax via dislocations after several layers were grown.

Despite the fact that the large volume required to create a direct gap in Si is probably unattainable, there are still interesting and potentially useful properties of Si which are obtained from this study. For example, there are two notable features in the variation of Si levels with volume. First, at high enough volume the gap will close and the system will metallize. This corresponds to metallization at a large *negative* pressure, in contrast to the usual process of metallization which occurs at positive pressures due to the  $\Gamma$ - $X$  overlap. The second feature is the triangle which is created by the variations of the  $L_1$ ,  $X_1$ , and  $\Gamma_{2'}$  levels with volume (from about 320 to 350 a.u.<sup>3</sup>). This feature is not specific to silicon, but occurs in Ge, Sn, and even SiSn.

In order to better understand the  $\Gamma_{2'}$  state's strong dependence on lattice expansion and the various crossings of the conduction-band states with volume, we decomposed the total band energy for the  $\Gamma_{25'}$ ,  $\Gamma_{2'}$ ,  $X_1$ , and  $L_1$  states into components arising from the local potential energy and from the kinetic energy.

The kinetic energy and local potential energy for Si as a function of volume are plotted in Figs. 2 and 3. The

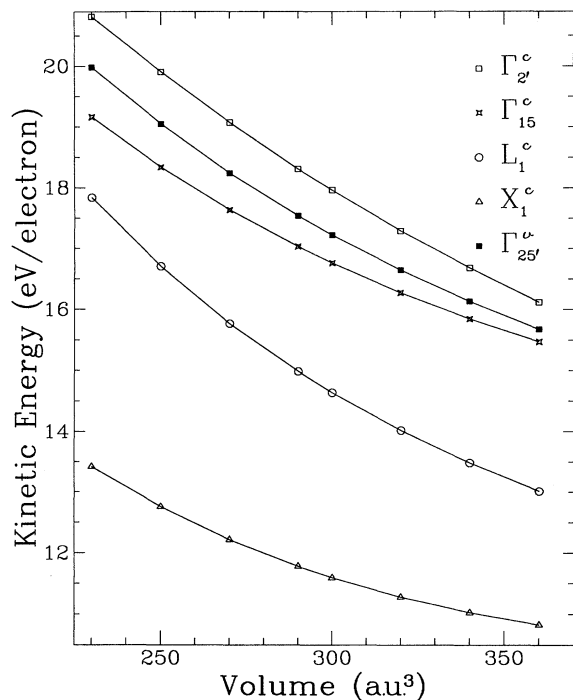


FIG. 2. The kinetic energy as a function of volume is shown for symmetry points in Si.

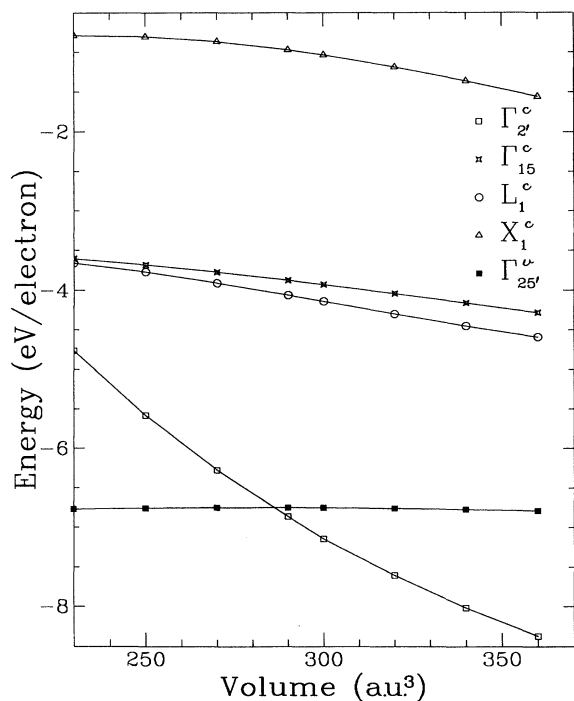


FIG. 3. The local potential energy as a function of volume is shown for symmetry points in Si.

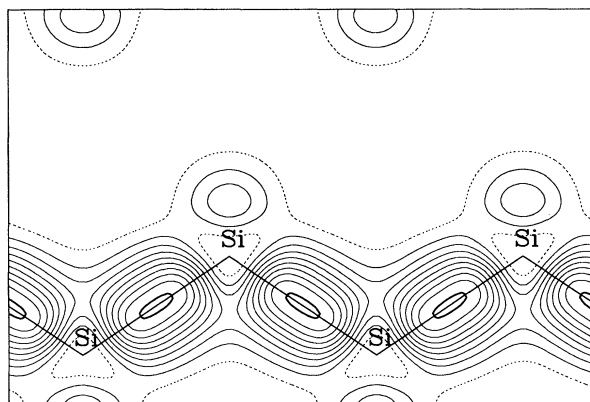


FIG. 4. Charge-density contours of the  $\Gamma_{25'}^v$  state in Si at the experimental equilibrium volume (270 a.u.<sup>3</sup>) are shown. The (110) plane is shown. Contours of 1, 2, ..., 10 electrons/unit cell are drawn. The lowest contour is shown as a dotted line, and the highest contour is shown as a bold line.

decrease in kinetic energy with increasing volume is similar for the  $L_1$  and  $\Gamma_{2'}$  states which have net decreases of about 4.8 and 4.7 eV, respectively, over the volume range studied. The  $\Gamma_{25'}^v$  and  $\Gamma_{15}^c$  states decrease by 4.3 and 3.7 eV, while the  $X_1^c$  state decreases by only 2.6 eV. Potential energies of the  $\Gamma_{15}^c$ ,  $X_1^c$ , and  $L_1^c$  levels drop by 0.5 eV or less over the volume range studied. The valence-band  $\Gamma_{25'}^v$  state shows a small rise in potential energy, but the conduction-band  $\Gamma_{2'}$  state's potential energy drops by more than 2.5 eV. A study of the charge-density distribution of these states helps to explain the overall ordering of the kinetic- and potential-energy levels.

Charge densities for the  $\Gamma_{25'}^v$ ,  $\Gamma_{15}^c$ ,  $\Gamma_{2'}$ ,  $X_1^c$ , and  $L_1^c$  states are given in Figs. 4–8. Although the states are shown only at the experimental equilibrium volume, their qualitative character changes little with lattice expansion. The top of the valence-band  $\Gamma_{25'}^v$  charge density is concentrated in the bonding region. This state has a highly localized charge density with a maximum  $\rho(r)$  of

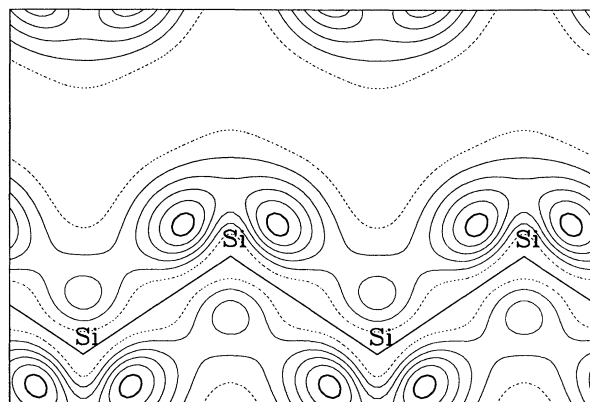


FIG. 5. Charge-density contours of the  $\Gamma_{15}^c$  state in Si. Contours of 1, 2, ..., 6 electrons/unit cell are drawn.

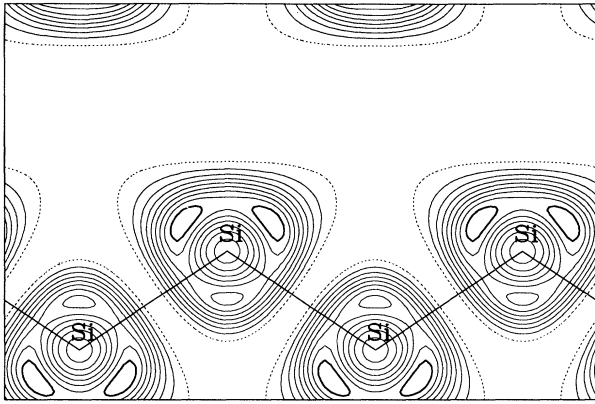


FIG. 6. Charge-density contours of the  $\Gamma_{2'}$  state in Si are shown. Contours of 1, 2, . . . , 10 electrons/unit cell are drawn.

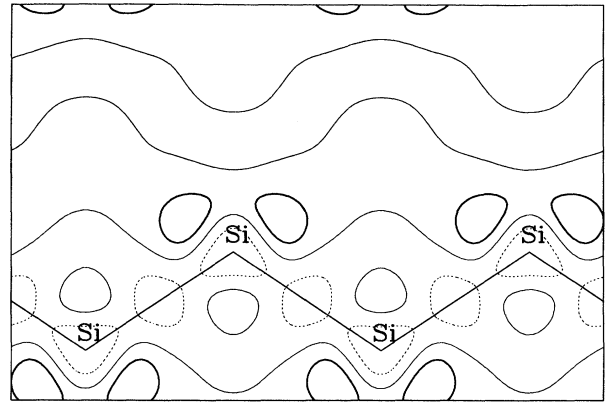


FIG. 8. Charge-density contours of the  $X_1$  state in Si are shown. Contours of 1, 2, and 3 electrons/unit cell are drawn.

about ten electrons per unit cell. At the equilibrium volume, the first  $\Gamma$  state in the conduction band is  $\Gamma_{15}$ . The charge density for this state, shown in Fig. 5, is much more spread-out than for the  $\Gamma_{25'}$  valence-band state. In contrast to the bonding maxima of the  $\Gamma_{25'}$  state, the  $\Gamma_{15}$  state has antibonding maxima.

Charge contours for the  $\Gamma_{2'}$  state in the conduction band are shown in Fig. 6. Like  $\Gamma_{15}$ , it has antibonding maxima, but the  $\Gamma_{2'}$  is much more localized with a maximum  $\rho(r)$  of about 9.75 electrons per unit cell. The first conduction band state at  $L$ ,  $L_1$ , is shown in Fig. 7. The charge distribution for  $L_1$  is very similar to the  $\Gamma_{2'}$  state, though much less concentrated with a maximum  $\rho(r)$  of about 6.4 electrons per unit cell. At  $X$ , the first conduction-band state is  $X_1$ . As shown in Fig. 8, it is the least localized state with a maximum  $\rho(r)$  of about 3.7 electrons per unit cell. It can be characterized as being spread out over the interstitial region.

By examining these charge densities, the relative ordering of the kinetic energies and their different variations with volume can be qualitatively explained. The "least localized" state  $X_1$  should and does have the lowest kinetic energy. The two states  $\Gamma_{2'}$  and  $\Gamma_{25'}$  which have

the highest kinetic energies also have the highest peaks in  $\rho(r)$ . Even though the  $L_1$  and  $\Gamma_{15}$  states have similar ranges in  $\rho(r)$ , the avoidance of interstitial regions by the  $\Gamma$  state raises its kinetic energy above  $L_1$ .

While the degree of localization explains the relative ordering of the states, the drops in kinetic energy for the five states plotted can be explained by examining the shape of the charge distributions. The  $\Gamma_{2'}$  and  $L_1$  states drop by about 4.75 eV over the volume range plotted in Fig. 2. These states both have spherical-like charge densities centered on the Si atoms. For the  $\Gamma_{25'}$  state, with charge concentrated between Si atoms, the drop in kinetic energy is 4.3 eV. Based on the maximum in  $\rho(r)$ ,  $\Gamma_{25'}$  has a very high absolute kinetic energy but its *volume dependence* is less strong than for  $\Gamma_{2'}$  and  $L_1$ . This is because with decreases in volume the charge in the  $\Gamma_{25'}$  state is free to relax perpendicular to the bond. Charge in the more spherical states does not have this freedom.

States with charge minima in the bond region such as  $\Gamma_{15}$  and  $X_1$  show the least kinetic-energy variation with volume. Kinetic-energy drops for these states are 3.70 and 2.60 eV, respectively. While both states are depleted along the Si-Si bonds, the  $\Gamma_{15}$  state is fairly localized near the atoms whereas the  $X_1$  state is spread uniformly in the interstitial region. Thus, changes in volume affect  $\Gamma_{15}$  slightly more than  $X_1$  although both states are less restricted in shape than the  $L_1$ ,  $\Gamma_{2'}$ , and  $\Gamma_{25'}$  states.

Ionic potentials for Si from about 15% below to about 33% above the equilibrium volume were studied. The change in potential in this volume range is basically from a directional potential, with large wells along the bonding directions, to a fairly spherically symmetric "atomiclike" potential. Variations in potential energies of the band edge states can be predicted based on their distributions of charge and the positions of the minima of the solid-state potential.

Charge-density maxima for the  $\Gamma_{25'}$  state lie in the middle of the bond and vary only slightly with lattice expansion. At very high volumes the charge density develops a "double hump" in the bond charge similar to carbon in the diamond structure. For the range of volumes studied, the charge distribution stays essentially

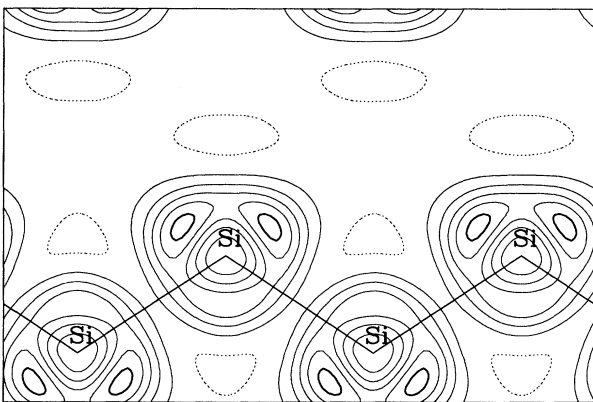


FIG. 7. Charge-density contours of the  $L_1$  state in Si are shown. Contours of 1, 2, . . . , 6 electrons/unit cell are drawn.

constant with a slight *decrease* in the maximum of  $\rho(r)$  as the unit-cell volume is increased. The double-hump character at high volume is an attempt to lower the state's potential energy by fitting into the atomiclike potential minima near the ions.

The  $\Gamma_{2'}$  state's maxima, however, lie along arcs around the ions fitting into the minimum of the potential. As the cell volume is increased, the maximum in  $\rho(r)$  increases from 8.8 to 11.2 electrons per unit cell at 230 a.u.<sup>3</sup> and 360 a.u.<sup>3</sup>, respectively. Separate atomiclike orbitals start to form around each ion. This is the primary reason for the dramatic decrease in potential energy with volume of the  $\Gamma_{2'}$  state. The  $\Gamma_{15}$ ,  $L_1$ , and  $X_1$  states also have maxima that can take advantage of the change in potential with volume. Although they are much less localized than the  $\Gamma_{2'}$  state these states also show increases in the peak value of  $\rho(r)$  with volume. Hence, their potential energies decrease with volume but at a rate much smaller than for the  $\Gamma_{2'}$  state.

Based on this discussion, one can explain why Si is an indirect semiconductor at the equilibrium volume. Although the  $\Gamma$  states in the conduction band have a low potential energy compared to the  $X_1$  state over a wide volume range, the high kinetic energy dominates at volumes around  $V_0$ . It is not until the  $\Gamma_{2'}$  state's charge density becomes strongly localized in the minimum of the solid's potential that it becomes lower in energy than the  $L_1$  or  $X_1$  states. Therefore the intrinsic size of the Si atoms determines  $V_0$  which forces the relative ordering of the states, causing the energy gap to be indirect.

The variation of the levels with volume (see shaded region of Fig. 1) shows an interesting pattern formed by the  $X$ ,  $L$ , and  $\Gamma$  levels as the gap changes from indirect at  $X$  to indirect at  $L$  to direct. There is a delicate balance between the decreases in kinetic and potential energies for the  $X_1$  and  $L_1$  states. Although the  $X_1$  state's potential energy drops slightly faster than the energy for  $L_1$ , the kinetic energy of the  $L_1$  state drops even faster as compared to  $X_1$  and thus the  $L_1$  state becomes the lowest conduction-band state for a small range of volumes. The  $\Gamma_{2'}$  state "passes" even the  $L_1$  state at high volumes because its drop in potential energy is so much larger than for  $L_1$ .

### Ge, Sn, and SiSn

To understand more generally the connection between variations in volume and potential of band states, we consider the  $\Gamma$ ,  $X$ , and  $L$  states for Ge and Sn (omitting the conduction-band  $\Gamma$  state analogous to the Si  $\Gamma_{15}$ ). The results are shown in Figs. 9 and 10. For comparison, we also calculated the energy levels for SiSn in the zinc-blende structure. The energy levels as a function of volume for SiSn are shown in Fig. 11.

In Ge the gap is from  $\Gamma$  to  $L$ , while Sn has a zero gap at the zone center ( $\Gamma_8$  is threefold degenerate, while  $\Gamma_7$  is nondegenerate). SiSn at the calculated equilibrium volume has an indirect gap from  $\Gamma$  to  $X$ , similar to Si. It is known that the trends in the energy gaps of the group-IV materials can be reproduced with changes in the ionic

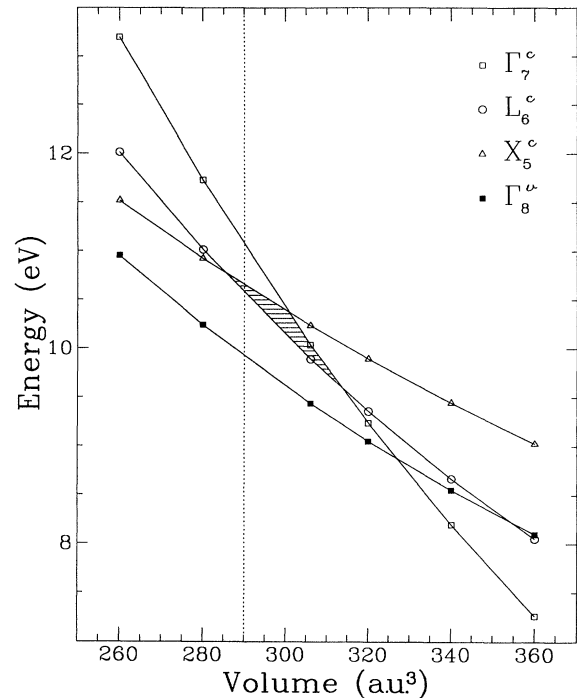


FIG. 9. Band-edge levels as a function of the primitive cell volume for Ge are shown. The calculated equilibrium volume is denoted by the dashed vertical line.

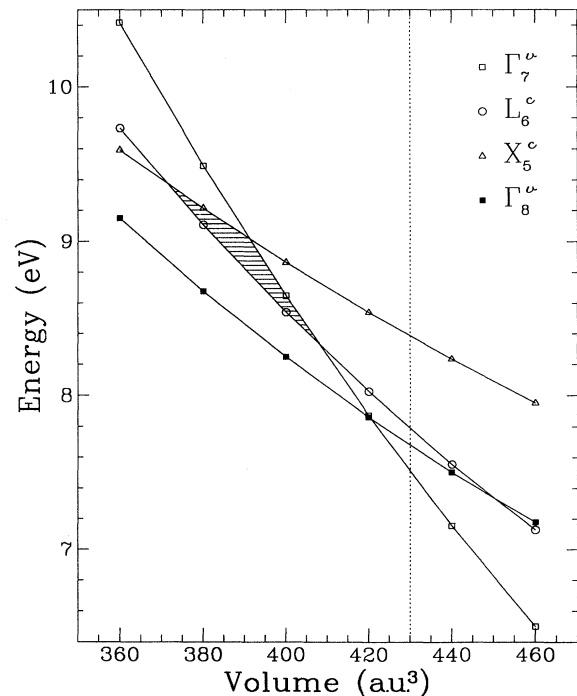


FIG. 10. Band-edge levels as a function of the primitive cell volume for Sn are shown. The calculated equilibrium volume is denoted by the dashed vertical line.

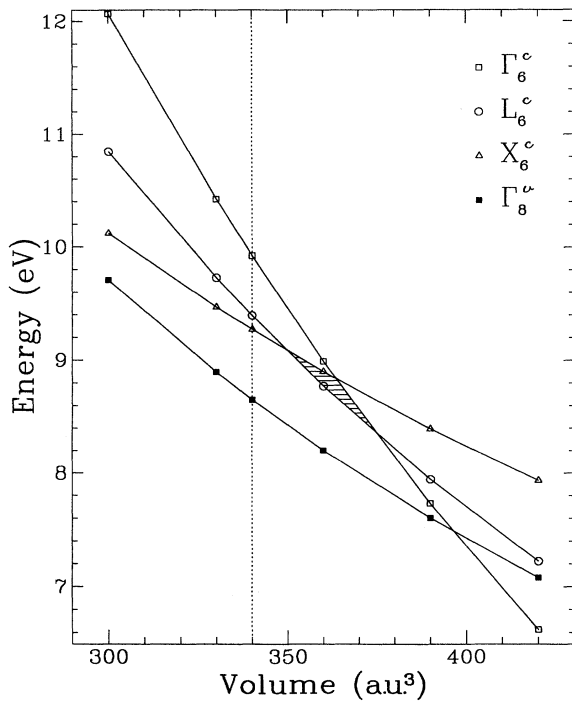


FIG. 11. Band-edge levels as a function of the primitive cell volume for zinc-blende SiSn are shown. The calculated equilibrium volume is denoted by the dashed vertical line.

potential.<sup>5</sup> However, the patterns in the dependence of Si levels on volume such as the “triangle” are unmistakably present in the variation of Ge, Sn, and even SiSn levels with volume. Hence, the gap in SiSn could be obtained

by expanding Si closer to the  $X_1-L_1$  crossing, and the indirect  $\Gamma \rightarrow L$  gap for Ge could be obtained by expanding Si past the  $X-L$  crossing. Even the zero gap of Sn could be obtained by expanding Si through the  $L-\Gamma$  crossing and until the conduction-band  $\Gamma$  state crossed the top of the valence band.

Although it is clear that the energy gap is determined by an interplay between the potential and the volume, the similarity in the dependence of the band-edge levels on volume for Si, Ge, Sn, and even SiSn suggests that volume alone may be an interesting parameter to vary. Changes in the potential just place the materials in different equilibrium positions on the “universal” energy-volume graph. By carefully controlling the composition of a IV-IV alloy, one could presumably find the area in potential-volume phase space where the gap is direct.

A theoretical study of  $\text{Ge}_{1-x}\text{Sn}_x$  alloys<sup>4</sup> showed that an alloy of  $\sim 70\%$  Ge,  $30\%$  Sn would yield a material with a direct gap of  $\sim 0.5$  eV. This gap is calculated to decrease with increasing Sn content and to close at  $x \simeq 0.74$ . This is consistent with our study. The stability of GeSn (Ref. 4) alloys and of SiGe (Ref. 13) alloys has been investigated, and these studies show that epitaxial films may be successfully grown despite the fact that the bulk materials are not expected to be stable.

#### ACKNOWLEDGMENTS

This work was supported by National Science Foundation Grant No. DMR91-20269 and by the Director, Office of Energy Research, Office of Basic Energy Sciences, Materials Science Division of the U.S. Department of Energy under Contract No. DE-AC03-76SF00098. J.L.C. acknowledges support from AT&T Bell Laboratories.

<sup>1</sup>L. T. Canham, *Appl. Phys. Lett.* **57**, 1046 (1990).

<sup>2</sup>S. B. Zhang and A. Zunger (unpublished); A. J. Read, R. J. Needs, K. J. Nash, L. T. Canham, P. D. J. Calcott, and A. Qteish, *Phys. Rev. Lett.* **69**, 1232 (1992); F. Buda, J. Kohanoff, and M. Parrinello, *ibid.* **69**, 1272 (1992).

<sup>3</sup>M. S. Hybertsen and M. Schlüter, *Phys. Rev. B* **36**, 9683 (1987); S. Froyen, D. M. Wood, and A. Zunger, *ibid.* **37**, 6893 (1988).

<sup>4</sup>K. A. Mäder, A. Baldereschi, and H. von Känel, *Solid State Commun.* **69**, 1123 (1989).

<sup>5</sup>C. Varea de Alvarez and M. L. Cohen, *Phys. Rev. B* **8**, 1603 (1973).

<sup>6</sup>D. R. Hamann, M. Schlüter, and C. Chiang, *Phys. Rev.*

*Lett.* **43**, 1494 (1979).

<sup>7</sup>J. P. Perdew and A. Zunger, *Phys. Rev. B* **23**, 5048 (1981).

<sup>8</sup>D. M. Ceperley and B. J. Alder, *Phys. Rev. Lett.* **45**, 566 (1980).

<sup>9</sup>D. J. Chadi and M. L. Cohen, *Phys. Rev. B* **8**, 5747 (1973).

<sup>10</sup>K. J. Chang, S. Froyen, and M. L. Cohen, *Solid State Commun.* **50**, 105 (1984); S. Fahy, K. J. Chang, S. G. Louie, and M. L. Cohen, *Phys. Rev. B* **35**, 5856 (1987).

<sup>11</sup>See, for example, J. Ihm, A. Zunger, and M. L. Cohen, *J. Phys. C* **12**, 4409 (1979).

<sup>12</sup>M. T. Yin and M. L. Cohen, *Phys. Rev. B* **29**, 12 (1984).

<sup>13</sup>J. L. Martins and A. Zunger, *Phys. Rev. Lett.* **56**, 1400 (1986).